

$H \rightarrow b\bar{b}$ in VBF at the LHC with an extra central photon^(*)

F. PICCININI

INFN, Sezione di Pavia - v. A. Bassi 6, I-27100 Pavia, Italy

(ricevuto il 10 Novembre 2009; pubblicato online il 18 Gennaio 2010)

Summary. — The LHC potential for a measurement of the Higgs boson coupling to the b -quark in the standard model is not well established yet. We show that requiring a large-transverse-momentum photon in the light Higgs boson production via vector-boson fusion (with subsequent $H \rightarrow b\bar{b}$ decay) could provide a further handle on the $Hb\bar{b}$ coupling determination, and on the measurement of the HWW coupling as well.

PACS 12.15.-y – Electroweak interactions.

PACS 12.15.Ji – Applications of electroweak models to specific processes.

1. – Introduction

Once the Higgs boson is discovered at the LHC, it will be crucial to test its properties, and check how well they fit in the standard model (SM) framework. Higgs boson couplings to vector bosons, heavy quarks and heavy leptons can in principle be measured by combining informations on different production and decay channels [1].

A measurement of the Higgs boson coupling to b quarks seems presently quite challenging. On the one hand, the SM Higgs production channel $b\bar{b} \rightarrow H$ is overwhelmed by the main production process $gg \rightarrow H$ at the LHC [2]. On the other hand, processes involving the $Hb\bar{b}$ coupling via the Higgs decay $H \rightarrow b\bar{b}$ (for $m_H \lesssim 140$ GeV) seem at the moment hard to manage, due to the large b (and, more generally, jet) background expected from pure QCD processes. The $H \rightarrow b\bar{b}$ decay in the Higgs production via vector-boson fusion (VBF) has been studied in [3]. It gives rise to four-jet final states, out of which two jets should be b -tagged. Although the VBF final states have quite distinctive kinematical features (*i.e.*, two forward jets with a typical transverse momentum of order M_W plus a resonant b -jet pair produced centrally), different sources of QCD backgrounds and hadronic effects presently make the relevance of this channel for a $Hb\bar{b}$ coupling determination difficult to assess. For instance, triggering on $b\bar{b}jj$ final states must confront

^(*) Based on work done in collaboration with Emidio Gabrielli, Fabio Maltoni, Barbara Mele, Mauro Moretti and Roberto Pittau.

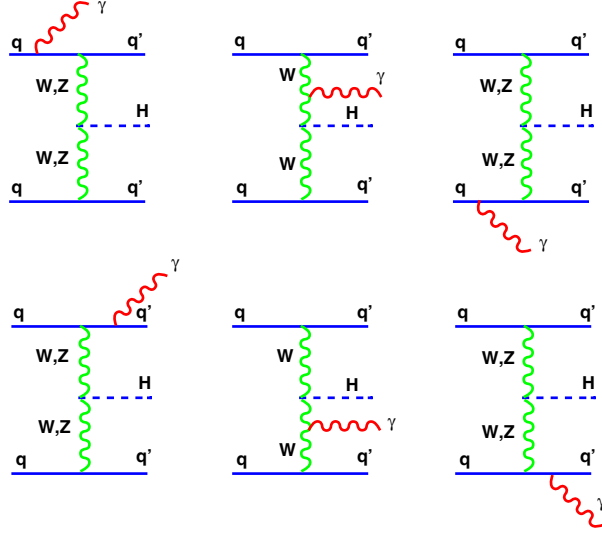


Fig. 1. – Tree-level t -channel Feynman diagrams for H production via $pp \rightarrow H \gamma jj$.

with the corresponding large QCD four-jet trigger rate. The $Ht\bar{t}$ associated production, where the Higgs boson is radiated by a top-quark pair, with subsequent $H \rightarrow b\bar{b}$ decay, could also provide a $Hb\bar{b}$ coupling measurement. Nevertheless, the recent inclusion of more reliable QCD background estimate and detector simulation in the corresponding signal analysis [4] have lowered the expectations on the potential of this channel.

Here we report on a further process that could help in determining the $Hb\bar{b}$ coupling, that was recently studied in [5] (where more details can be found). We consider the Higgs boson production in VBF in association with a large-transverse-momentum photon (*i.e.*, $p_T \gtrsim 20$ GeV) emitted centrally (*i.e.*, with pseudorapidity $|\eta_\gamma| < 2.5$)

$$(1) \quad pp \rightarrow H \gamma jj + X \rightarrow b\bar{b} \gamma jj + X,$$

where H decays to $b\bar{b}$, and, at the parton level, the final QCD partons are identified with the corresponding jets j . Disregarding the resonant contribution to the process coming from the $WH\gamma$, $ZH\gamma$ production, the dominant Feynman diagrams are the ones involving VBF (as shown in fig. 1, where the Higgs decay to $b\bar{b}$ is not shown). Final states $b\bar{b} \gamma jj$ arising from photon radiation off one of the two b -quarks arising from the Higgs boson decay (via $pp \rightarrow H(\rightarrow b\bar{b} \gamma) jj$) fall outside the experimental $m_{b\bar{b}}$ resolution window around the m_H , due to the requirement of a large- p_T photon.

2. – Benefits from the central photon

Adding a central photon to the $pp \rightarrow H(\rightarrow b\bar{b}) jj$ final state, despite a further e.m. fine-structure constant α that depletes production rates, gives a number of benefits [5]:

- first of all, the presence of an additional high- p_T photon can improve the triggering efficiencies for multi-jet final states, such as those needed to select $pp \rightarrow H(\rightarrow b\bar{b}) jj$ events;

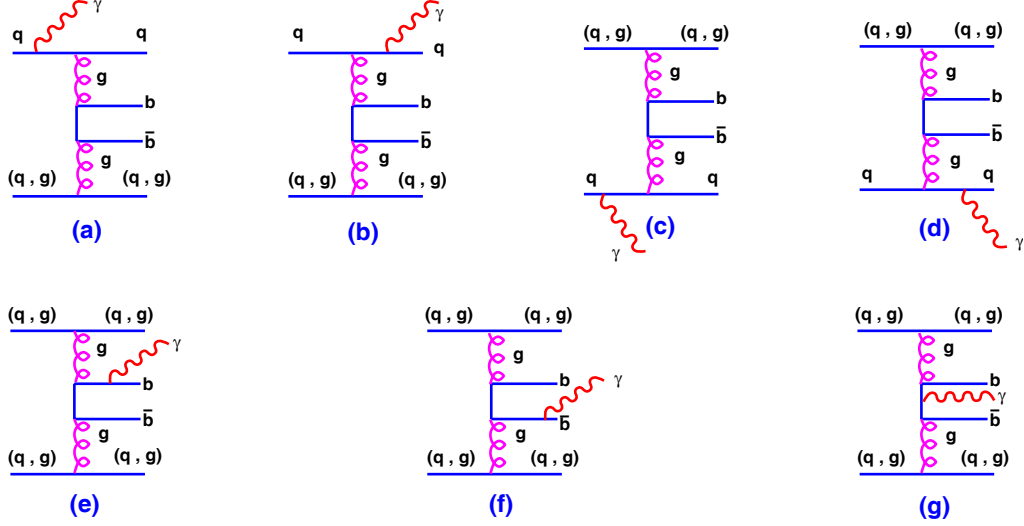


Fig. 2. – Representative classes of Feynman diagrams contributing, at parton level, to the background process $pp \rightarrow b\bar{b}\gamma jj$. Here q and g stand for a light quark (u, d, s) and gluons, respectively.

- there is a large gluonic component entering the partonic processes giving rise to the QCD backgrounds to the $b\bar{b}\gamma jj$ final state, as shown in fig. 2; as a consequence, the QCD backgrounds are in general much less *active* in radiating a large- p_T photon with respect to the VBF signal;
- further dynamical *coherence* effects dramatically suppress the radiation of a photon in the irreducible QCD background to $b\bar{b}\gamma jj$, when the photon is central (*i.e.* emitted outside the typical radiation cone around the initial/final quark legs, for quarks scattered in the t -channel);
- a similar *coherence* effect depletes the HZZ amplitudes (involving neutral currents) with the respect to the HWW ones (involving charged currents) in fig. 1, increasing the relative sensitivity to the HWW coupling in the radiative channel; then, a measurement of the $b\bar{b}\gamma jj$ rate could lead to a combined determination of the Higgs boson couplings to b quarks and W vector bosons, with less contamination from the HZZ coupling uncertainties;
- the requirement of a central photon strongly reduces the background arising from alternative Higgs boson production processes, such as the one coming from the virtual gluon fusion $g^*g^* \rightarrow H$ diagrams, with a photon radiated off any external quark leg.

In the following, we will elaborate on a few of the previous items.

3. – Production rates: signal *versus* background

In table I, the cross-sections for the signal and irreducible background for the process in eq. (1) are shown for three values of the Higgs boson mass, as independently obtained by the Monte Carlo event generators ALPGEN [6], and MadEvent [7], with the choice of

TABLE I. – Cross-sections for the signal and the irreducible background for the optimized event selection, as defined in eq. (2). The signal and irreducible background production rates for the plain VBF process are also shown, with the same event selection.

m_H	120 GeV	130 GeV	140 GeV
$\sigma[H(\rightarrow b\bar{b})\gamma jj]$	3.6 fb	2.9 fb	2.0 fb
$\sigma[b\bar{b}\gamma jj]$	33 fb	38 fb	40 fb
$\sigma[H(\rightarrow b\bar{b})jj]$	320 fb	255 fb	168 fb
$\sigma[b\bar{b}jj]$	103 pb	102 pb	98 pb

parameters described in [5]. The following event selection, that optimizes the significance S/\sqrt{B} , has been applied:

$$(2) \quad \begin{aligned} p_T^{j1,b1} &\geq 60 \text{ GeV}, & p_T^{j2,b2} &\geq 30 \text{ GeV}, & p_T^\gamma &\geq 20 \text{ GeV}, \\ \Delta R_{ik} &\geq 0.7, & |\eta_\gamma| &\leq 2.5, & |\eta_b| &\leq 2.5, \\ |\eta_j| &\leq 5, & m_{jj} &> 800 \text{ GeV}, & m_H(1 - 10\%) &\leq m_{b\bar{b}} \leq m_H(1 + 10\%), \\ |\Delta\eta_{jj}| &> 4, & m_{\gamma H} &\geq 160 \text{ GeV}, & \Delta R_{\gamma b/\gamma j} &\geq 1.2, \end{aligned}$$

where ik is any pair of partons in the final state, and $\Delta R_{ik} = \sqrt{\Delta^2\eta_{ik} + \Delta^2\phi_{ik}}$, with η the pseudorapidity and ϕ the azimuthal angle. For comparison, cross-sections and irreducible background for the plain VBF process are also shown.

The above optimized event selection has been obtained by generating events according to the basic event selection

$$(3) \quad \begin{aligned} p_T^j &\geq 30 \text{ GeV}, & p_T^b &\geq 30 \text{ GeV}, & \Delta R_{ik} &\geq 0.7, \\ |\eta_\gamma| &\leq 2.5, & |\eta_b| &\leq 2.5, & |\eta_j| &\leq 5, \\ m_{jj} &> 400 \text{ GeV}, & m_H(1 - 10\%) &\leq m_{b\bar{b}} \leq m_H(1 + 10\%), \\ p_T^\gamma &\geq 20 \text{ GeV}, \end{aligned}$$

and maximizing the significance on the differential distributions

$$\frac{d\sigma}{dm_{jj}}, \quad \frac{d\sigma}{dp_T^{j1}}, \quad \frac{d\sigma}{dp_T^{b1}}, \quad \frac{d\sigma}{dm_{\gamma H}}, \quad \frac{d\sigma}{|\Delta\eta_{jj}|},$$

where $j1$ and $b1$ denote the leading p_T light jet and b -jet, respectively, and $m_{\gamma H}$ is the invariant mass of the $\gamma b\bar{b}$ system.

In case the usual pattern of QED corrections held, the request of a further hard photon would keep the relative weight of signal and background unchanged with respect to the $pp \rightarrow H jj$ case. Indeed, the rates for $pp \rightarrow H \gamma jj$ and its background would be related to a $\mathcal{O}(\alpha)$ rescaling of the rates for the $H jj$ signal and its background, respectively, keeping the S/B ratio approximately stable. On the other hand, both the $H \gamma jj$ signal and its background statistics would decrease according to the rescaling factor $\mathcal{O}(\alpha)$. Consequently, if $(S/\sqrt{B})|_{H(\gamma)jj}$ is the signal significance for the VBF process (with) without a central photon, the signal significance for $pp \rightarrow H \gamma jj$ would fall down as $(S/\sqrt{B})|_{H\gamma jj} \sim \sqrt{\alpha} (S/\sqrt{B})|_{Hjj} \lesssim 1/10 (S/\sqrt{B})|_{Hjj}$ with respect to the basic VBF

TABLE II. – Statistical significances with the optimized event selection as defined in eq. (2), for an integrated luminosity of 100 fb^{-1} . The value $\epsilon_b = 60\%$ for the b -tagging efficiency and a Higgs boson event reduction by $\epsilon_{b\bar{b}} \simeq 70\%$, due to the finite ($\pm 10\%$) $b\bar{b}$ mass resolution, are assumed. Jet-tagging efficiency and photon identification efficiency are set to 100%. Only the irreducible background is included in B .

m_H	120 GeV	130 GeV	140 GeV
$S/\sqrt{B} _{H\gamma jj}$	2.6	2.0	1.3
$S/\sqrt{B} _{H jj}$	3.5	2.8	1.9

process. This would question the usefulness of considering the $H\gamma jj$ variant of the Hjj process, apart from the expected improvement in the triggering efficiency of the detectors due to the lower background rates.

In table I, one can see that the QED naive expectations do not necessarily apply when restricted regions of phase space are considered (as discussed in detail in [5]). We see that the naive QED rescaling fails for the main background processes $pp \rightarrow b\bar{b}(\gamma)jj$, whose rate drops by about a factor 3000 after requiring a central photon, due to destructive interference (*coherence*) effects discussed in [5]. Since, on the other hand, the signal cross-section roughly follows the naive QED rescaling $\sigma_\gamma \sim \sigma/100$, the requirement of a central photon gives rise to a dramatic increase (by more than one order of magnitude) in the S/B ratio. Indeed, in table II, comparable statistical significances for the signal with and without a photon are obtained, for an integrated luminosity of 100 fb^{-1} .

In order to have a sensible estimate of the achievable S/B ratio and statistical significance at parton level, we computed in [5] with ALPGEN the cross-sections, assuming $m_H = 120 \text{ GeV}$ and with the optimized event selection of eq. (2), for three main potentially dangerous processes⁽¹⁾:

- $pp \rightarrow \gamma + 4$ jets, where two among the light jets are fake tagged as b -jets;
- $pp \rightarrow b\bar{b} + 3$ jets, where one of the light jets is misidentified as a photon;
- $pp \rightarrow 5$ jets, where one of the light jets is misidentified as a photon, and two light jets are fake tagged as b -jets.

The cross-sections quoted in table III should then be multiplied by the appropriate efficiencies: ϵ_{fake}^2 for $pp \rightarrow \gamma + 4$ jets, $\epsilon_b^2 \epsilon_{\gamma j}$ for $pp \rightarrow b\bar{b} + 3$ jets and $3 \epsilon_{\text{fake}}^2 \epsilon_{\gamma j}$ for $pp \rightarrow 5$ jets, where ϵ_{fake} is the efficiency of mistagging a light jet as a b -jet, and $\epsilon_{\gamma j}$ is the rejection factor of a jet against a photon. Assuming $\epsilon_{\text{fake}} = 1\%$ and $\epsilon_{\gamma j} = 1/5000$ ⁽²⁾, one can see that the reducible backgrounds do not perturb dramatically the significancies of table II.

Apart from enhancing the S/B ratio, coherence effects in $pp \rightarrow H(\rightarrow b\bar{b})\gamma jj$ remarkably curb the relative contribution of the $ZZ \rightarrow H$ boson fusion diagrams with respect to the $WW \rightarrow H$ ones. In order to prove this last statement, we selected, among all possible subprocesses contributing to $pp \rightarrow H(\gamma)jj$, a first set of subprocesses (named N) mediated only by the ZZ fusion, namely $qq \rightarrow H(\gamma)qq$ (in particular, we summed up cross-sections for $q = (u, d, s, c, \bar{u}, \bar{d}, \bar{s}, \bar{c})$), and a second set of subprocesses (named C)

⁽¹⁾ We estimated that the process $p\bar{p} \rightarrow c\bar{c}\gamma jj$, where the c -quarks are both mistagged as b -quarks, (assuming $\epsilon_c = 10\%$) can be safely neglected.

⁽²⁾ This is the value quoted in [8], see also [9].

TABLE III. – Cross-sections for reducible background channels, for the optimized event selection (2). The value $m_H = 120$ GeV is assumed.

Process	$p_T^\gamma \geq 20$ GeV
$\sigma(pp \rightarrow \gamma + 4j)$	2.27(2) pb
$\sigma(pp \rightarrow b\bar{b} + 3j)$	61.1(3) pb
$\sigma(pp \rightarrow 5j)$	2.40(1) nb

mediated only by the WW fusion (in this case, we summed up the 8 cross-sections of the type $u\bar{c} \rightarrow H(\gamma) d\bar{s}$). Calling $\sigma^{(N,C)}$ the cross-sections for the two latter sets, we computed the following ratios among the radiative and the non-radiative processes at the LHC:

$$\frac{\sigma^{(N)}(H\gamma jj)}{\sigma^{(N)}(H jj)} = 0.0016, \quad \frac{\sigma^{(C)}(H\gamma jj)}{\sigma^{(C)}(H jj)} = 0.013,$$

where we applied the cuts $p_T^\gamma \geq 20$ GeV, $|\eta_\gamma| \leq 2.5$, and $\Delta R_{j\gamma} \geq 0.7$, assuming $m_H = 120$ GeV. It is then clear that the radiation is suppressed in the presence of the HZZ vertex.

Thanks to the above feature, the $H(\rightarrow b\bar{b})\gamma jj$ production at the LHC can have a role not only in the determination of the Hbb coupling, but also for a cleaner determination of the HWW coupling.

The analysis presented above does not include parton shower effects. The latter are expected to further differentiate the signal and background final-state topology and composition. A preliminary analysis of showering and central-jet veto effects points to an improvement of S/\sqrt{B} by about a factor two [5]. The inclusion of complete showering, hadronization, and detector simulations will be needed to establish the actual potential of the process $pp \rightarrow H(\rightarrow b\bar{b})\gamma jj$.

* * *

I wish to thank G. CHIARELLI, M. GRECO and G. ISIDORI and for their kind invitation. Pleasant and fruitful collaboration with E. GABRIELLI, F. MALTONI, B. MELE, M. MORETTI and R. PITTAU is acknowledged.

REFERENCES

- [1] See, for instance, REINA L., arXiv:hep-ph/0512377.
- [2] HAHN T., HEINEMEYER S., MALTONI F., WEIGLEIN G. and WILLENBROCK S., arXiv:hep-ph/0607308.
- [3] MANGANO M. L., MORETTI M., PICCININI F., PITTAU R. and POLOSA A. D., *Phys. Lett. B*, **556** (2003) 50 [arXiv:hep-ph/0210261].
- [4] CUCCIARELLI S. *et al.*, CERN-CMS-NOTE-2006-119.
- [5] GABRIELLI E., MALTONI F., MELE B., MORETTI M., PICCININI F. and PITTAU R., *Nucl. Phys. B*, **781** (2007) 64 [arXiv:hep-ph/0702119].
- [6] MANGANO M. L., MORETTI M., PICCININI F., PITTAU R. and POLOSA A. D., *JHEP*, **0307** (2003) 001 [arXiv:hep-ph/0206293].
- [7] MALTONI F. and STELZER T., *JHEP*, **0302** (2003) 027 [arXiv:hep-ph/0208156].
- [8] ESCALIER M., DERUE F., FAYARD L., KADO M., LAFORGE B., REIFEN C. and UNAL G., ATL-PHYS-PUB-2005-018.
- [9] PIERI M., ARMOURT K. and BRANSON J. G., CERN-CMS-Note-2006-007.